# Supplementary information

## TAO-kinase 3 governs the terminal differentiation of NOTCH2-dependent splenic conventional dendritic cells

Matthias Vanderkerken[1,2], Bastiaan Maes[1,2], Lana Vandersarren[1,2], Wendy Toussaint[1,2], Kim Deswarte[1,2], Manon Vanheerswynghels[1,2], Philippe Pouliot[1,2], Liesbet Martens[3], Sofie Van Gassen[3], Connie M. Arthur[4], Margaret E. Kirkling[5], Boris Reizis[5], Daniel Conrad[6], Sean Stowell[4], Hamida Hammad[1,2,*], Bart N. Lambrecht[1,2,7,*]

1. VIB Center for Inflammation Research, 9000 Ghent, Belgium.
2. Department of Internal Medicine and Pediatrics, Ghent University, 9000 Ghent, Belgium
3. Department of Biomedical Molecular Biology, Ghent University, 9000 Ghent, Belgium.
4. Department of Pathology and Laboratory Medicine, Center for Transfusion Medicine and Cellular Therapies, Emory University School of Medicine, Atlanta, GA 30322, USA.
5. Department of Pathology, New York University School of Medicine, New York, NY 10016, USA.
6. Center for Clinical and Translational Research, Virginia Commonwealth University, Richmond, Virginia, VA 23298, USA.
7. Department of Pulmonary Medicine, Erasmus Medical Center, 3015 GD, Rotterdam, the Netherlands.

* These authors contributed equally

Correspondence may be addressed to: matthias.vanderkerken@ugent.be or bart.lambrecht@ugent.vib.be

www.pnas.org/cgi/doi/10.1073/pnas.2009847117

**Fig. S1**

a Marker expression per cluster

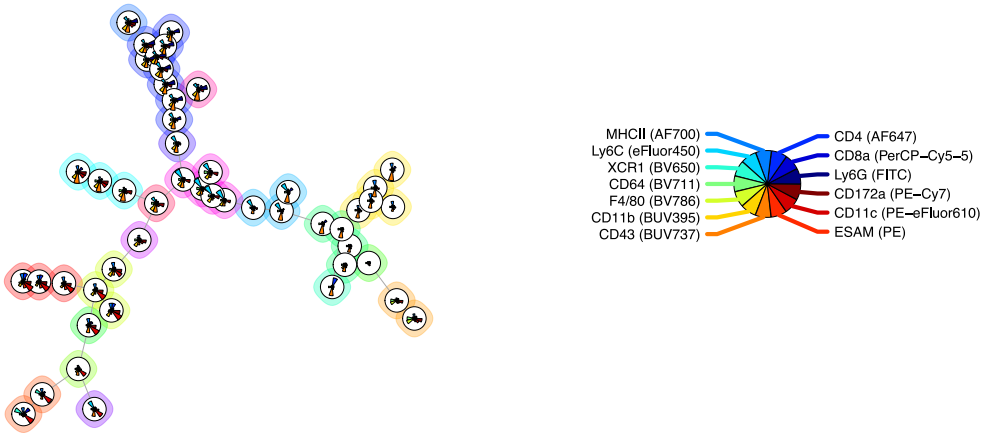


b Manual gating

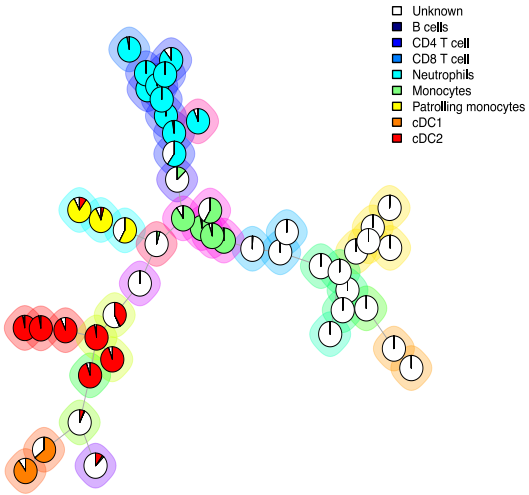


c Cluster IDs

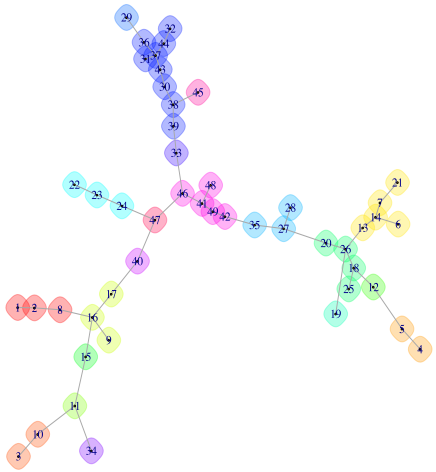

d

| Cluster ID | P value | Adjusted P value | Significant | Direction | Fold change |
|---|---|---|---|---|---|
| 1 | 0,007936508 | 0,019444444 | * | Decreasing | 43,51244122 |
| 2 | 0,007936508 | 0,019444444 | * | Decreasing | 10,1509232 |
| 38 | 0,007936508 | 0,019444444 | * | Increasing | 4,66215475 |
| 39 | 0,007936508 | 0,019444444 | * | Increasing | 4,317453273 |
| 27 | 0,007936508 | 0,019444444 | * | Increasing | 4,154799838 |
| 16 | 0,007936508 | 0,019444444 | * | Increasing | 3,694792143 |
| 28 | 0,007936508 | 0,019444444 | * | Increasing | 3,63693641 |
| 33 | 0,007936508 | 0,019444444 | * | Increasing | 3,167140698 |
| 45 | 0,007936508 | 0,019444444 | * | Increasing | 3,146737615 |
| 20 | 0,007936508 | 0,019444444 | * | Increasing | 2,867964739 |
| 32 | 0,015873016 | 0,033816425 | * | Increasing | 2,604843003 |
| 21 | 0,007936508 | 0,019444444 | * | Increasing | 2,520339219 |
| 29 | 0,007936508 | 0,019444444 | * | Increasing | 2,468688992 |
| 43 | 0,007936508 | 0,019444444 | * | Increasing | 2,36474443 |
| 31 | 0,015873016 | 0,033816425 | * | Decreasing | 2,328399169 |
| 7 | 0,007936508 | 0,019444444 | * | Increasing | 2,22889992 |
| 9 | 0,007936508 | 0,019444444 | * | Decreasing | 2,019360085 |
| 30 | 0,007936508 | 0,019444444 | * | Increasing | 1,971743667 |
| 40 | 0,007936508 | 0,019444444 | * | Decreasing | 1,852614436 |
| 23 | 0,015873016 | 0,033816425 | * | Decreasing | 1,739608672 |
| 4 | 0,007936508 | 0,019444444 | * | Decreasing | 1,699646997 |
| 42 | 0,007936508 | 0,019444444 | * | Decreasing | 1,67485317 |
| 35 | 0,007936508 | 0,019444444 | * | Increasing | 1,522063405 |

**Supplementary figure 1: Identification of a cDC2 deficit in *Taok3*$^{-/-}$ mice using the unsupervised clustering algorithm FlowSOM**

**(a-c)** FlowSOM tree generated from concatenated data from *Taok3*$^{+/+}$ and *Taok3*$^{-/-}$ splenocytes as described in Figure 1a and in materials and methods. Background colors denote the different metaclusters. **(a)** Pie charts indicate the expression of the indicated markers for each node. **(b)** Pie charts indicate the cellular composition of each node as determined by classical, manual gating. **(c)** FlowSOM tree with cluster identification numbers. **(d)** Table of Mann-Whitney U test results for the comparison of cluster frequencies between *Taok3*$^{+/+}$ and *Taok3*$^{-/-}$ mice. P values were adjusted using the Bonferroni correction for multiple comparisons. Only significantly differing clusters are listed, ranked by magnitude of fold change. The 'direction' label indicates whether cluster frequency is increased or decreased in *Taok3*$^{-/-}$ mice compared to littermate controls. Two-tailed Mann-Whitney U test. Data are representative of 2 biologically independent experiments (n=8-9 mice per group). The FlowSOM algorithm was run 5 times to ensure reproducibility of the results. * = $p<0.05$

**Fig. S2**

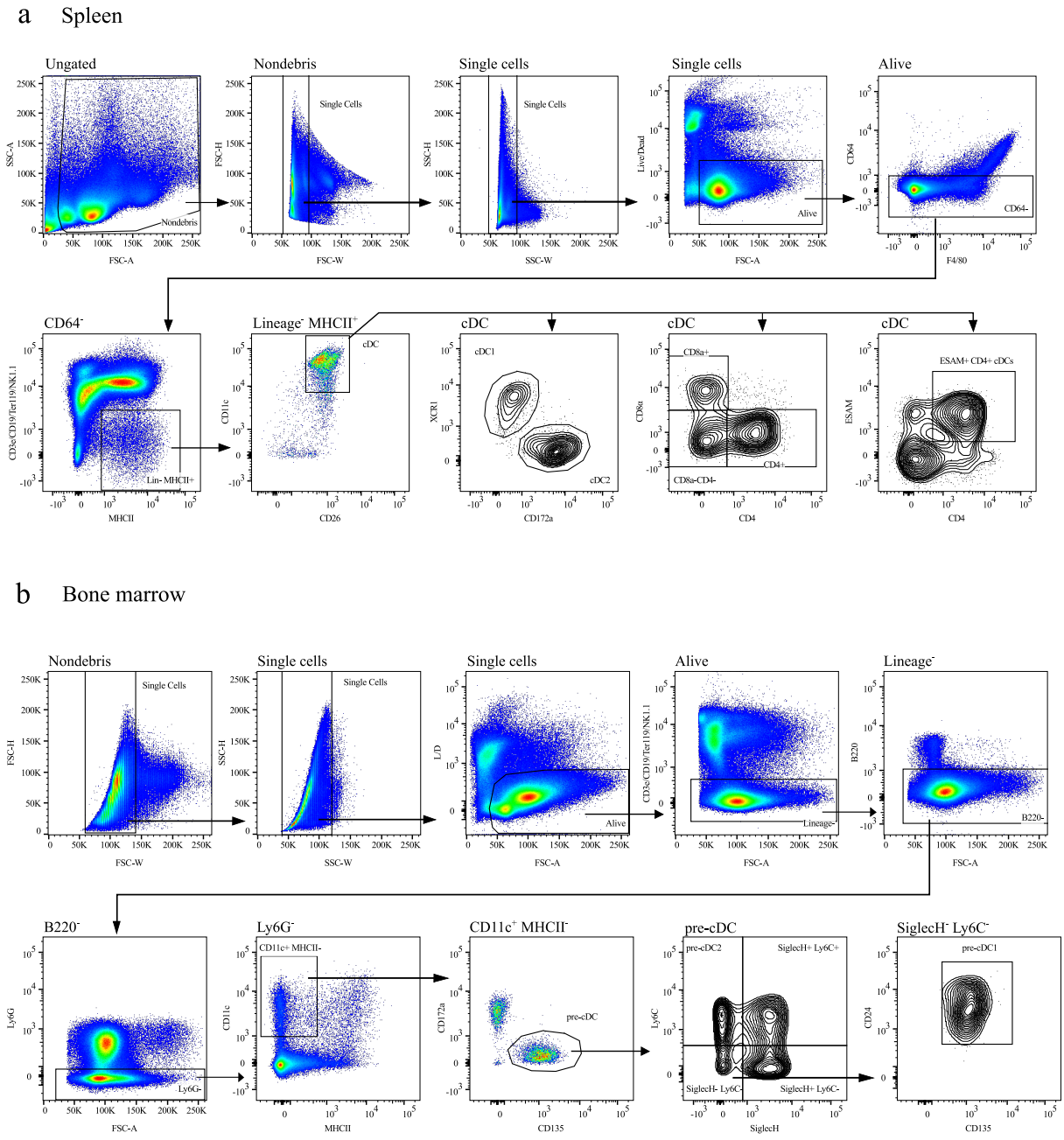


**Supplementary figure 2: Gating strategy for cDCs and pre-cDCs.**
**(a)** Gating strategy for conventional dendritic cells. In the spleen, cDCs are defined as single, live, CD64$^-$ lineage (CD3e/CD19/Ter119/NK1.1)$^-$ MHCII$^+$ CD11c$^{hi}$ CD26$^+$ cells. Type 1 cDCs (cDC1s) are defined as XCR1$^+$ CD172a$^-$, type 2 cDCs (cDC2s) as XCR1$^-$ CD172a$^+$. Alternative gating of cDC subsets based on CD4, CD8α and ESAM expression is shown. The gating strategy for cDCs lung, liver, small intestine and lymph nodes is similar but includes a CD45$^+$ gate. In lymph nodes, resident cDCs are identified as CD11c$^{hi}$ MHCII$^+$, migratory cDCs as CD11c$^+$ MHCII$^{hi}$ **(b)** Gating strategy for pre-cDCs. Pre-cDCs are defined as single, alive, lineage (CD3e/CD19/Ter119/NK1.1)$^-$ B220$^-$ Ly6G$^-$ CD11c$^{int/+}$ MHCII$^{lo}$ CD172$^{lo/int}$ CD135$^+$ cells. Among pre-cDCs, SiglecH$^+$ Ly6C$^-$ and SiglecH$^+$

Ly6C$^{+}$ cells contain both cDC1 and cDC2 potential. Pre-cDC1s are defined as SiglecH$^{-}$ Ly6C$^{-}$ CD24$^{hi}$ pre-cDCs, pre-cDC2s as SiglecH$^{-}$ Ly6C$^{+}$ pre-cDCs. Gating is shown for bone marrow but is similar for pre-cDCs in spleen.

**Fig. S3**

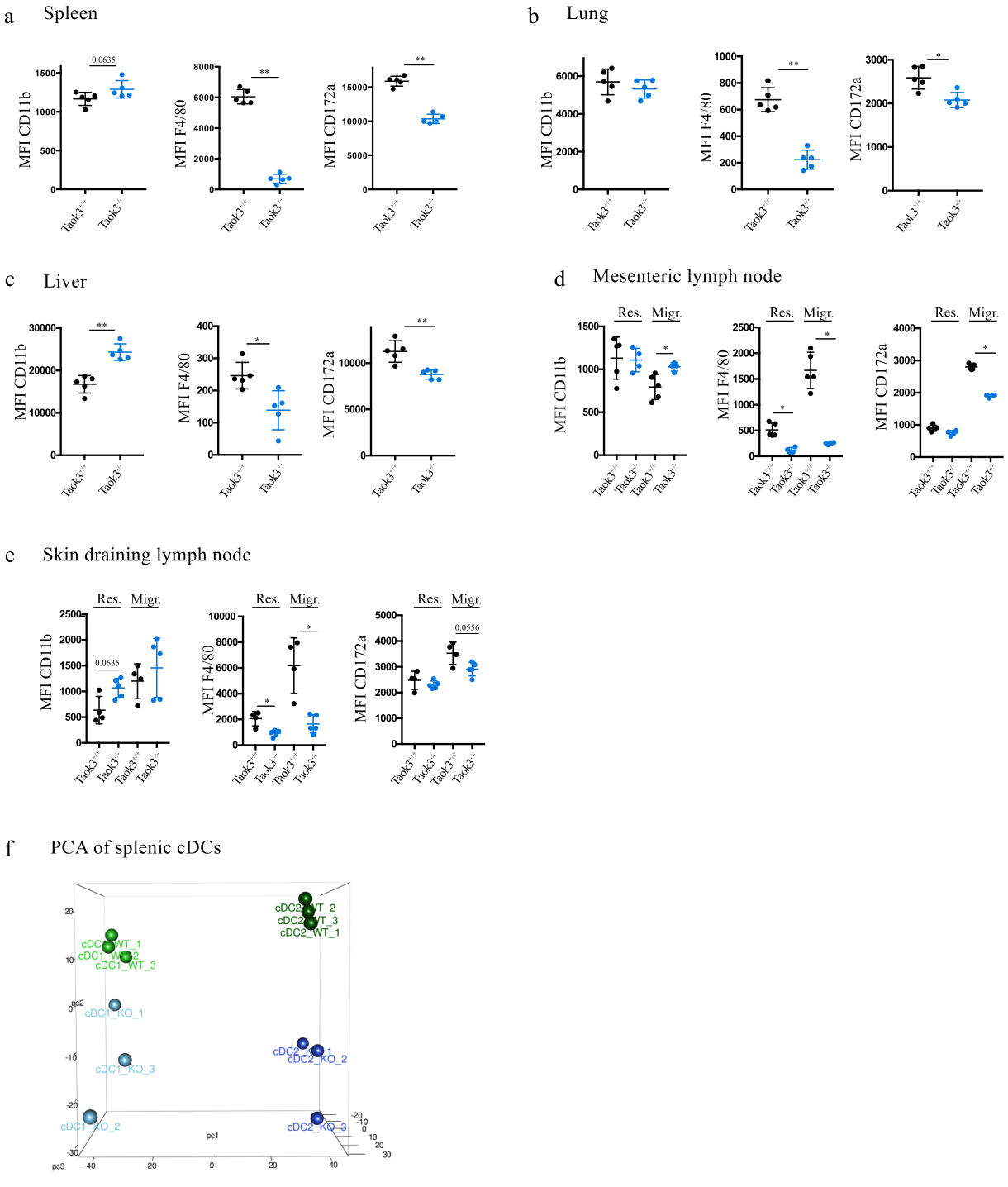


**Supplementary figure 3: Loss of *Taok3* alters the phenotype of cDC2s across different tissues.**

**(a-e)** Surface expression levels of CD11b, F4/80 and CD172a on splenic cDC2s in the spleen **(a)**, lung **(b)**, liver **(c)**, mesenteric lymph nodes **(d)** and skin-draining lymph nodes **(e)** from *Taok3*$^{-/-}$ mice (blue) or littermate controls (black), as determined by flow cytometry. 'Res.' and 'Migr.' denote resident and migratory cDC populations, respectively. Data representative of at least 2 independent experiments (n=8-12 per

group (a-d), or representative of 4-5 mice per group (e). Two-tailed Mann-Whitney U test. **(f)** Principal component analysis of cDNA microarray on sorted splenic cDC1s and cDC2s from *Taok3*$^{-/-}$ and *Taok3*$^{+/+}$ mice. Dendritic cells were sorted from 3 mice per group. Bars indicate mean ± SD. * = $p<0.05$, ** = $p<0.01$, *** = $p<0.001$, **** = $p<0.0001$.

**Fig. S4**

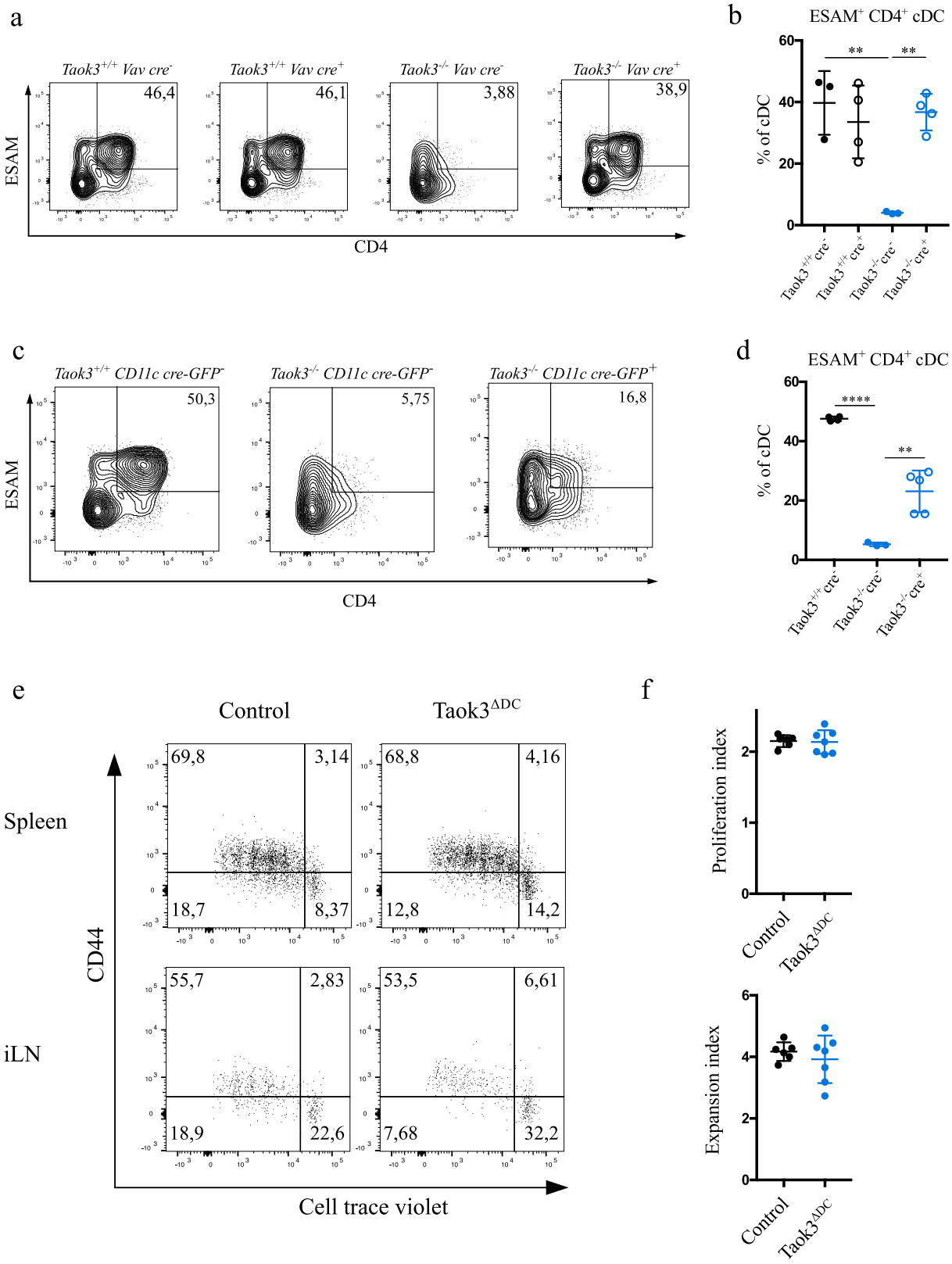
a
Taok3+/+ Vav cre-
Taok3+/+ Vav cre+
Taok3-/- Vav cre-
Taok3-/- Vav cre+
46,4
46,1
3,88
38,9
ESAM
CD4
b
ESAM+ CD4+ cDC
% of cDC
**
**
Taok3+/+ cre-
Taok3+/+ cre+
Taok3-/- cre-
Taok3-/- cre+
c
Taok3+/+ CD11c cre-GFP-
Taok3-/- CD11c cre-GFP-
Taok3-/- CD11c cre-GFP+
50,3
5,75
16,8
ESAM
CD4
d
ESAM+ CD4+ cDC
% of cDC
****
**
Taok3+/+ cre-
Taok3-/- cre-
Taok3-/- cre+
e
Control
Taok3ΔDC
Spleen
iLN
CD44
69,8
3,14
18,7
8,37
68,8
4,16
12,8
14,2
55,7
2,83
18,9
22,6
53,5
6,61
7,68
32,2
Cell trace violet
f
Proliferation index
Control
Taok3ΔDC
Expansion index
Control
Taok3ΔDC

**Supplementary figure 4: Selective gene trap reversal of *Taok3* in dendritic cells rescues cDC2 differentiation.**

**(a)** Representative contour plots of splenic cDCs from *Taok3*$^{+/+}$ Vav cre-, *Taok3*$^{+/+}$ Vav cre+, *Taok3*$^{-/-}$ Vav cre- and *Taok3*$^{-/-}$ Vav cre+ mice. **(b)** Percentage of ESAM$^{+}$ CD4$^{+}$ cells among cDCs. One-way ANOVA with Tukey's post-hoc test. Data in (a) and (b) are representative of 3-4 mice per group. **(c)** Representative contour plots of splenic cDCs from *Taok3*$^{+/+}$ CD11c cre-GFP-, *Taok3*$^{-/-}$ CD11c cre-GFP- and *Taok3*$^{-/-}$ CD11c cre-GFP+ mice. **(d)** Percentage of ESAM$^{+}$ CD4$^{+}$ cells among cDCs. One-way ANOVA with Tukey's post-hoc test. Data are representative of at least 2 independent experiments (n=8 per group). Numbers within the gate in (a) and (c) denote the percentage of total cDCs. **(e-f)** *Taok3*$^{\Delta DC}$ and littermate control mice were injected with CTV-labeled OTII-specific CD4$^{+}$ T cells and transfused with 100µl of HOD-RBCs 1 day later. **(e)** Representative dot plots of OTII cells in the spleen and inguinal lymph node (iLN) of control (left) and *Taok3*$^{\Delta DC}$ (right) acceptor mice 72h after HOD-RBC transfusion. Plots are pre-gated on live, CD19$^{-}$ NK1.1$^{-}$ Ter119$^{-}$ CD3e$^{+}$ CD4$^{+}$ CD45.1$^{+}$ cells. Numbers adjacent to the gates indicate the percentage of OTII cells. **(f)** Proliferation and expansion index of OTII cells in the spleen of acceptor mice, according to the Flowjo proliferation algorithm. Two-tailed Mann-Whitney U test. Data are representative of 7-8 mice per group. Bars indicate mean ± SD. * = $p<0.05$, ** = $p<0.01$, *** = $p<0.001$, **** = $p<0.0001$.

**Fig. S5**

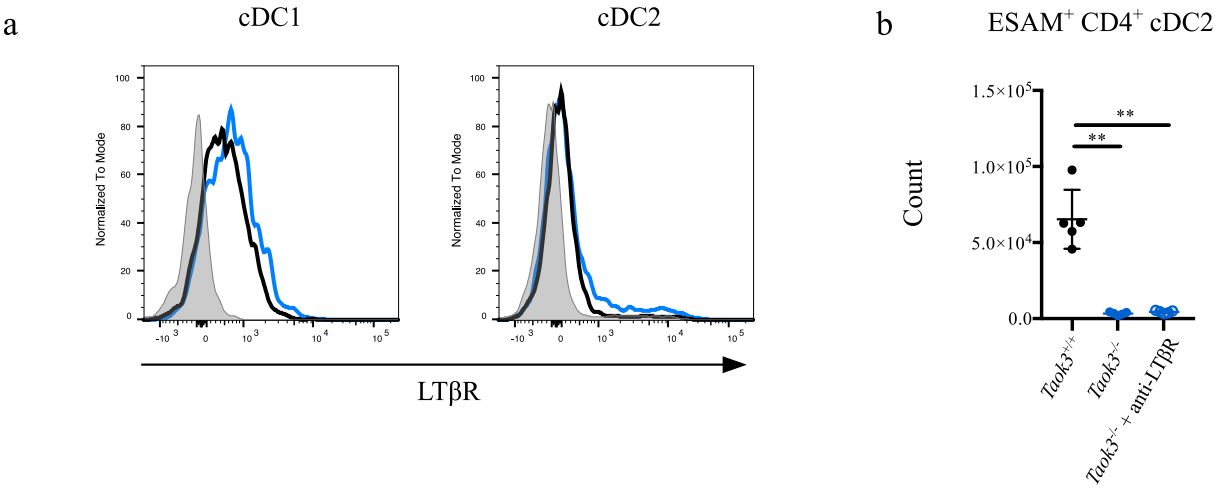


**Supplementary figure 5: The ESAM⁺ CD4⁺ cDC2 deficit in *Taok3*$^{-/-}$ mice is not restored by LTβR agonism.**
**(a)** Surface expression of the lymphotoxin β receptor on splenic cDC1s and cDC2s from *Taok3*$^{-/-}$ mice (blue) and littermate controls (black). An FMO for LTβR staining is shown in grey. Data representative of 2 independent experiments (n=8 per group). **(b)** Number of ESAM⁺ CD4⁺ cDC2s in the spleen of wild type mice (black), *Taok3*$^{-/-}$ mice, and *Taok3*$^{-/-}$ mice that were treated with an agonistic LTβR antibody for two weeks (see materials and methods). Data representative of 4-5 mice per group. Bars indicate mean ± SD. * = p<0.05, ** = p<0.01, *** = p<0.001, **** = p<0.0001.

# Fig. S6

a Downregulated genes in *Notch2*$^{-/-}$ cDC1 versus preranked cDC1 gene list

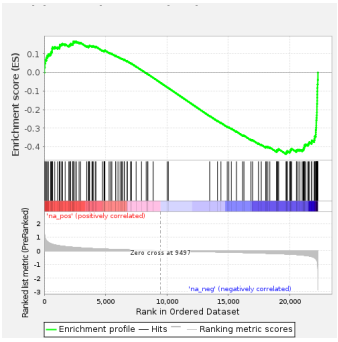


ES: -0.44
p<0.001

b Upregulated genes in *Notch2*$^{-/-}$ cDC1 versus preranked cDC1 gene list

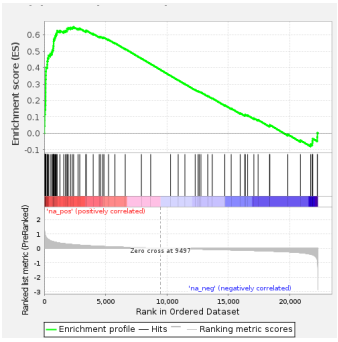


ES: 0.65
p<0.001

c Downregulated genes in *Notch2*$^{-/-}$ cDC2 versus preranked cDC2 gene list

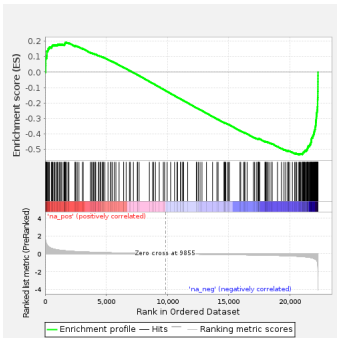


ES: -0.53
p<0.001

d Upregulated genes in *Notch2*$^{-/-}$ cDC2 versus preranked cDC2 gene list

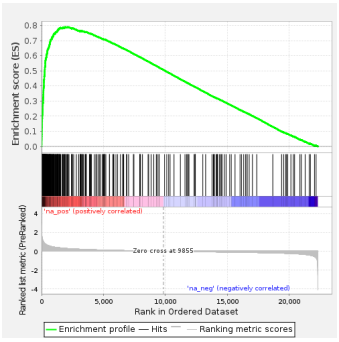


ES: 0.79
p<0.001

e

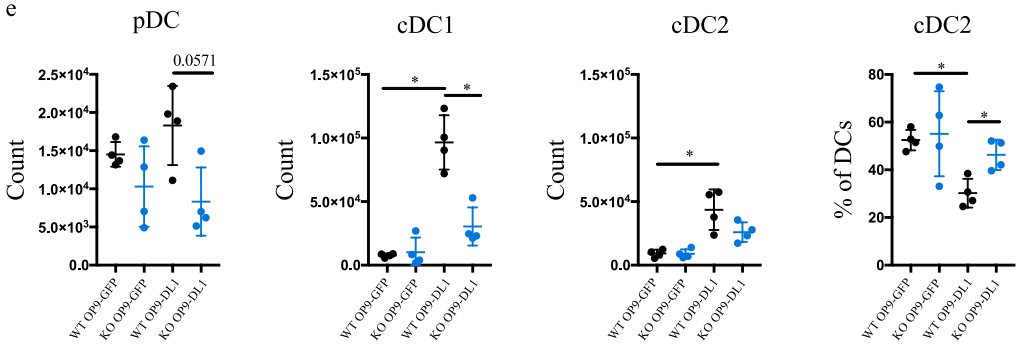


f

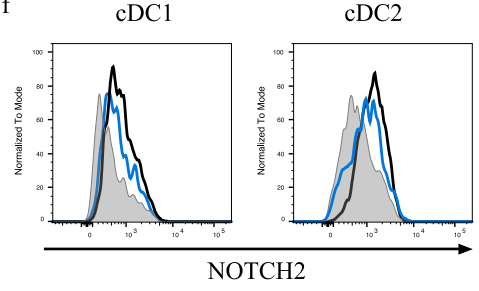


g

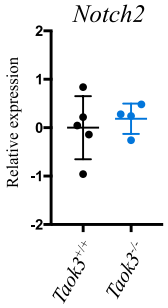


h

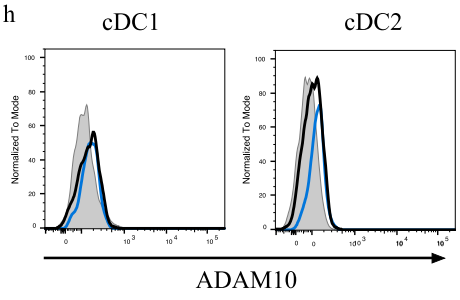

**Supplementary figure 6: The transcriptomes of *Notch2*-deficient and *Taok3*-deficient dendritic cells overlap significantly.**

**(a-d)** Gene transcripts from the cDNA microarray (see Fig. 1h) were ranked according to their fold change in *Taok3*$^{-/-}$ versus *Taok3*$^{+/+}$ cDC1s (a, b) and cDC2s (c, d). Gene set enrichment analysis (GSEA) was performed using a publically available set of genes that are differentially expressed in *Notch2*$^{-/-}$ versus wild type splenic cDCs (GSE45681). The enrichment plots for genes that are downregulated or upregulated in *Notch2*$^{-/-}$ cDC1s are displayed in **(a)** and **(b)**, respectively. The enrichment plots for genes that are downregulated or upregulated in *Notch2*$^{-/-}$ cDC2s are displayed in **(c)** and **(d)**, respectively. Enrichment scores (ES) and p-values are listed under each plot. **(e)** Yield of pDCs, cDC1s and cDC2s and percentage of cDC2s among alive cells in cocultures of *Taok3*$^{-/-}$ or *Taok3*$^{+/+}$ BM-derived DCs with OP-DL1 fibroblasts. One-way ANOVA with Tukey's post-hoc test. Data are representative of 2 independent experiments (9 biological replicates per group). **(f)** Surface expression of NOTCH2 on splenic cDC1s and cDC2s from *Taok3*$^{-/-}$ mice (blue) and littermate controls (black). An FMO is shown in grey. **(g)** mRNA levels of *Notch2* in sorted cDC2s sorted from *Taok3*$^{-/-}$ mice and littermate controls. Two-tailed Mann-Whitney U test. **(h)** Surface expression of ADAM10 on splenic cDC1s and cDC2s from *Adam10*$^{\Delta DC}$ mice (blue) and littermate controls (black). An FMO is shown in grey. (f-h) Data representative of at least2 independent experiments (n=8-10 per group). Bars indicate mean ± SD. * = $p<0.05$, ** = $p<0.01$, *** = $p<0.001$, **** = $p<0.0001$.

**Fig. S7**

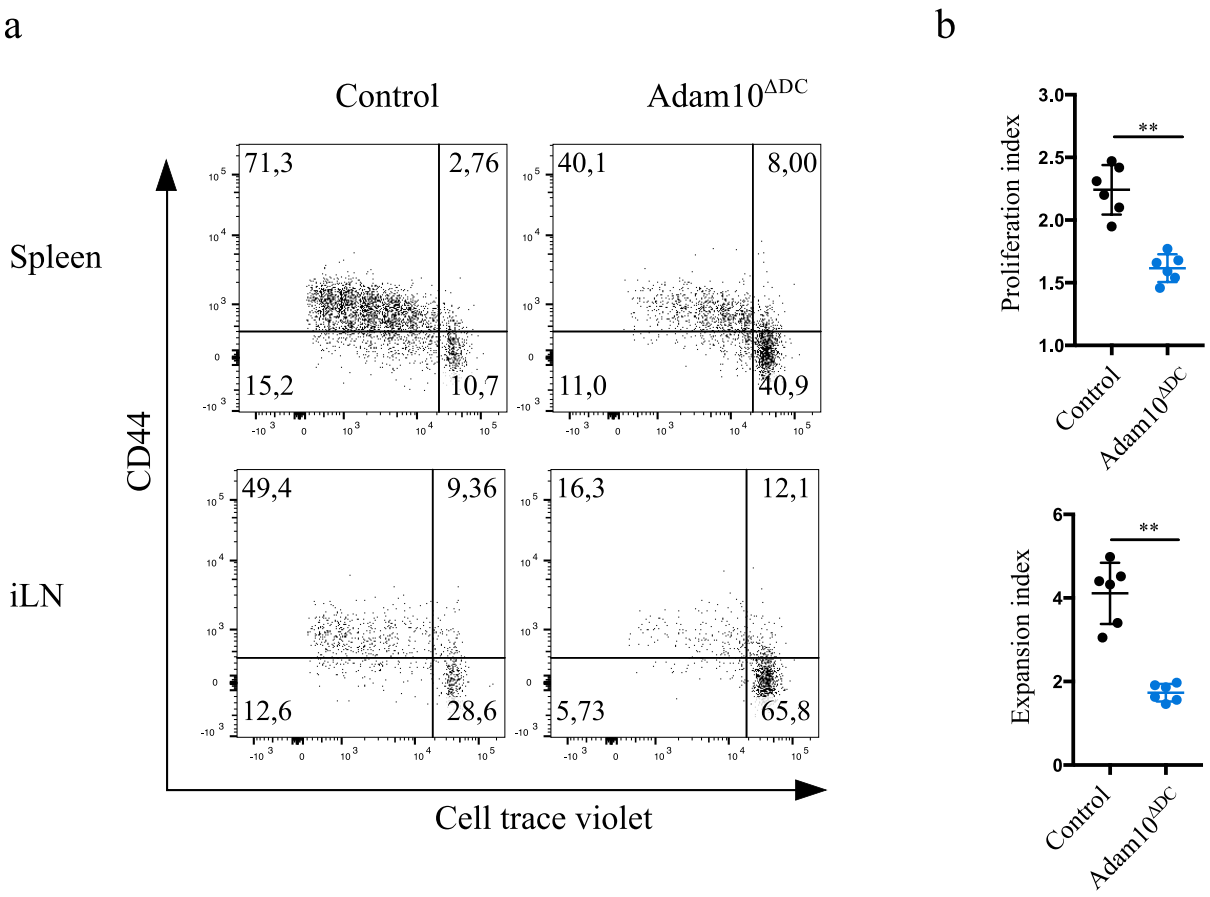


**Supplementary figure 7: CD4⁺ T cell priming against allogeneic red blood cells is impaired in *Adam10*$^{\Delta DC}$ mice.**
**(a-b)** *Adam10*$^{\Delta DC}$ and littermate control mice were injected with CTV-labeled OTII-specific CD4⁺ T cells and transfused with 100µl of HOD-RBCs 1 day later. **(a)** Representative dot plots of OTII cells in the spleen and inguinal lymph node (iLN) of control (left) and *Adam10*$^{\Delta DC}$ (right) acceptor mice 72h after HOD-RBC transfusion. Plots are pre-gated on live, CD19⁻ NK1.1⁻ Ter119⁻ CD3e⁺ CD4⁺ CD45.1⁺ cells. Numbers adjacent to the gates indicate the percentage of OTII cells. **(b)** Proliferation and expansion index of OTII cells in the spleen of acceptor mice, according to the Flowjo proliferation algorithm. Two-tailed Mann-Whitney U test. Data are representative of 7-8 mice per group. Bars indicate mean ± SD. * = p<0.05, ** = p<0.01, *** = p<0.001, **** = p<0.0001.

**Fig. S8**

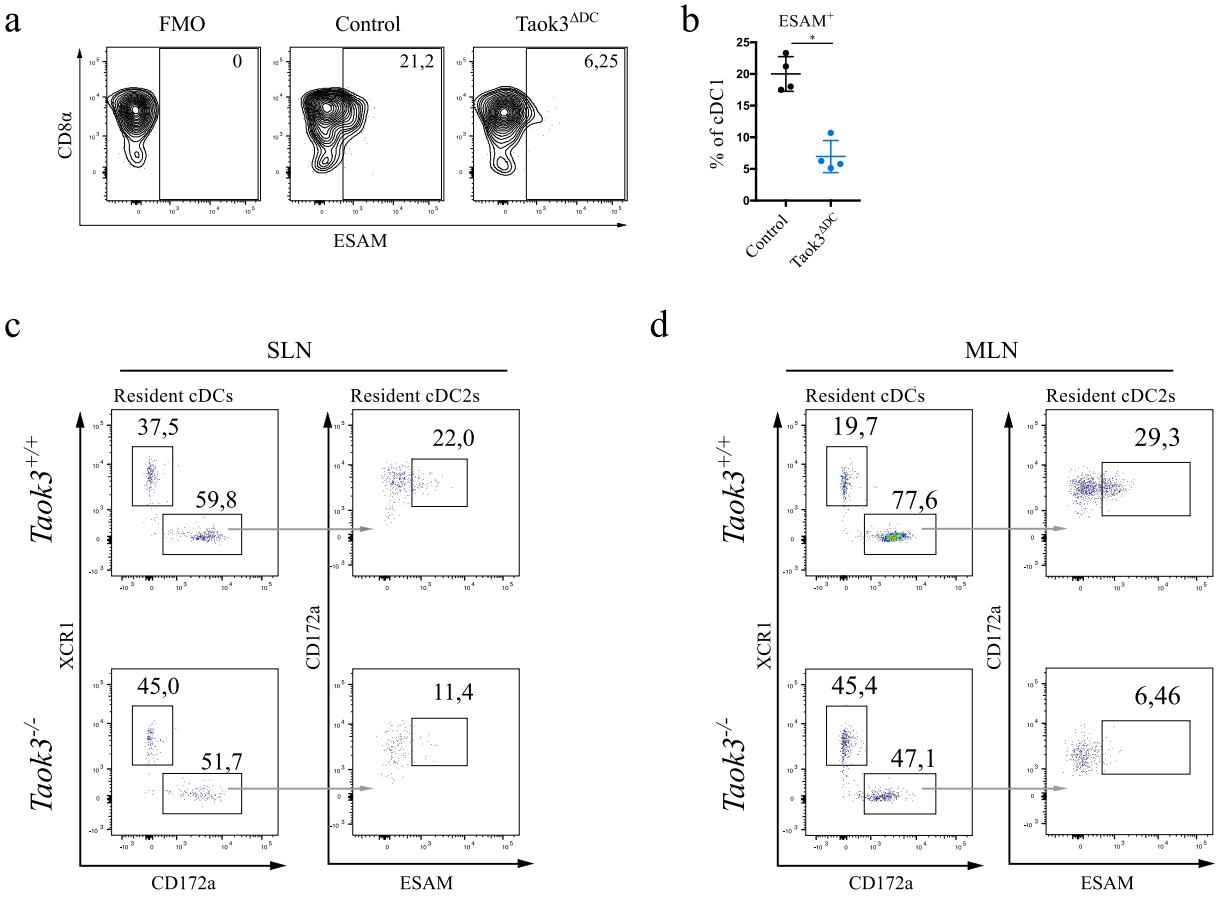


**Supplementary figure 8: *Taok3* controls ESAM expression in resident lymphoid tissue dendritic cells.**

**(a)** Representative plots of CD8α and ESAM expression on XCR1$^+$ splenic cDC1s from Taok3$^{\Delta DC}$ mice and littermate controls. A fluorescence minus one (FMO) control for ESAM staining is depicted. **(b)** Percentage of splenic cDC1s that express ESAM. (a, b) Data representative of 4 mice per group. Two sided Mann-Whitney U test. **(c, d)** Representative flow plots of resident cDCs (gated as single, live, CD45$^+$ lineage (CD3e/CD19/Ter119/NK1.1)$^-$ CD64$^-$ CD11c$^{hi}$ MHCII$^+$ cells) in skin-draining lymph nodes (SLN) (c) and mesenteric lymph nodes (MLN) (d) from *Taok3*$^{-/-}$ mice and littermate controls. Data are representative of 5 mice per group. Numbers adjacent to the gates indicate percentages of the parent population (a, c, d). Bars indicate mean ± SD. * = p<0.05, ** = p<0.01, *** = p<0.001, **** = p<0.0001.

**Fig. S9**

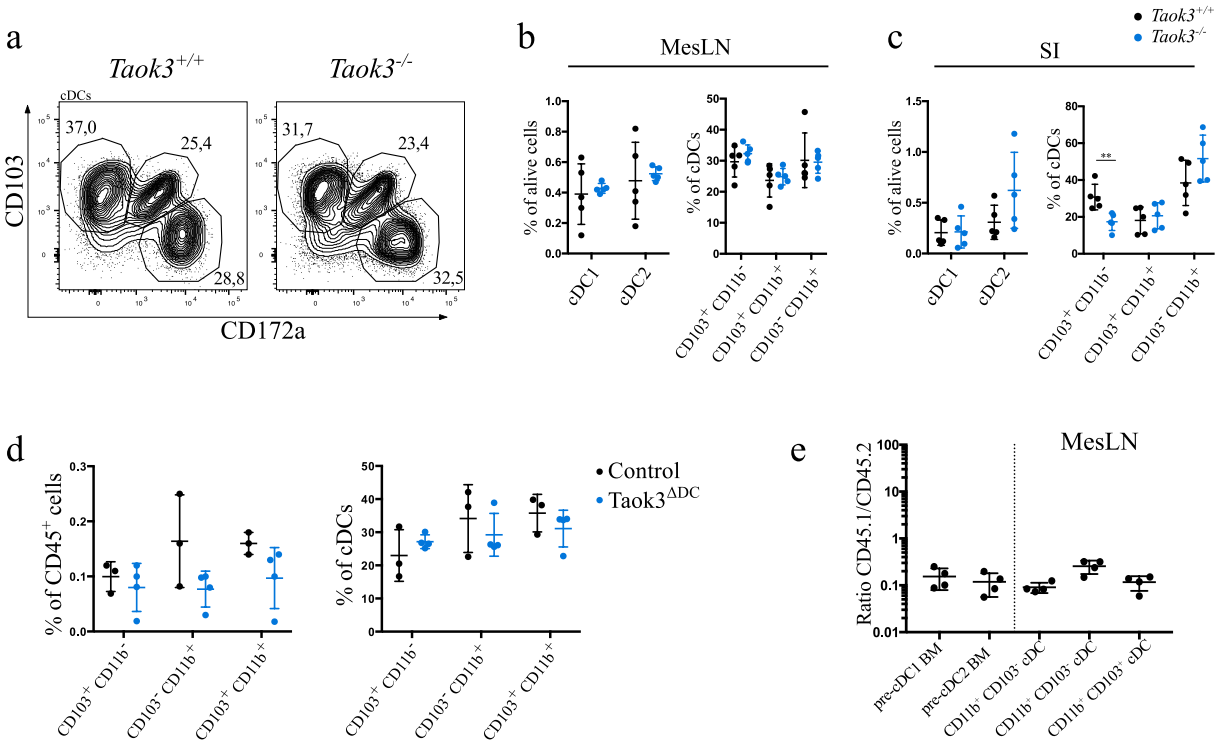


**Supplementary figure 9: Development of intestinal CD103⁺ CD11b⁺ cDCs does not rely on *Taok3*.**

**(a)** Representative contour plots of cDCs from mesenteric lymph nodes of *Taok3*$^{+/+}$ and *Taok3*$^{-/-}$ mice. Plots are pre-gated on live, CD45⁺ lineage (CD3e, CD19, NK1.1)$^{-}$ CD64$^{-}$ CD11c⁺ MHCII⁺ cells. **(b, c)** Frequency of cDC1 and cDC2 among live cells (left) and frequency of CD103⁺ CD11b$^{-}$, CD103⁺ CD11b⁺ and CD103$^{-}$ CD11b⁺ cells among cDCs (right) in mesenteric lymph node (MesLN) and in the lamina propria of the small intestine (SI). Two-tailed Mann-Whitney U test. Data in (a) and (b) are representative of 3 independent experiments (n=10-12 per group), data in (c) are representative of 2 independent experiments (n=7-8). Numbers adjacent to gates indicate the percentage of total cDCs. **(d)** Frequency of cDC subsets among CD45⁺ cells (left) and among total cDCs (right) in mesenteric lymph node of Taok3$^{\Delta DC}$ mice and littermate controls. Two-tailed Mann-Whitney U test. Data are representative of 3-4 mice per group. **(e)** Wild type acceptor mice were lethally irradiated and transplanted with mixed CD45.1 WT:CD45.2 *Taok3*$^{-/-}$ bone marrow in a 1:1 ratio. Contributions of CD45.1 and CD45.2 bone marrow to BM pre-cDCs and mature cDCs in mesenteric lymph nodes of acceptor mice 10 weeks after reconstitution are presented as CD45.1/CD45.2 ratios. One-way ANOVA with Bonferroni correction for multiple testing. Data are representative of 5 acceptor mice. Bars indicate mean ± SD. * = p<0.05, ** = p<0.01, *** = p<0.001, **** = p<0.0001.

**Fig. S10**

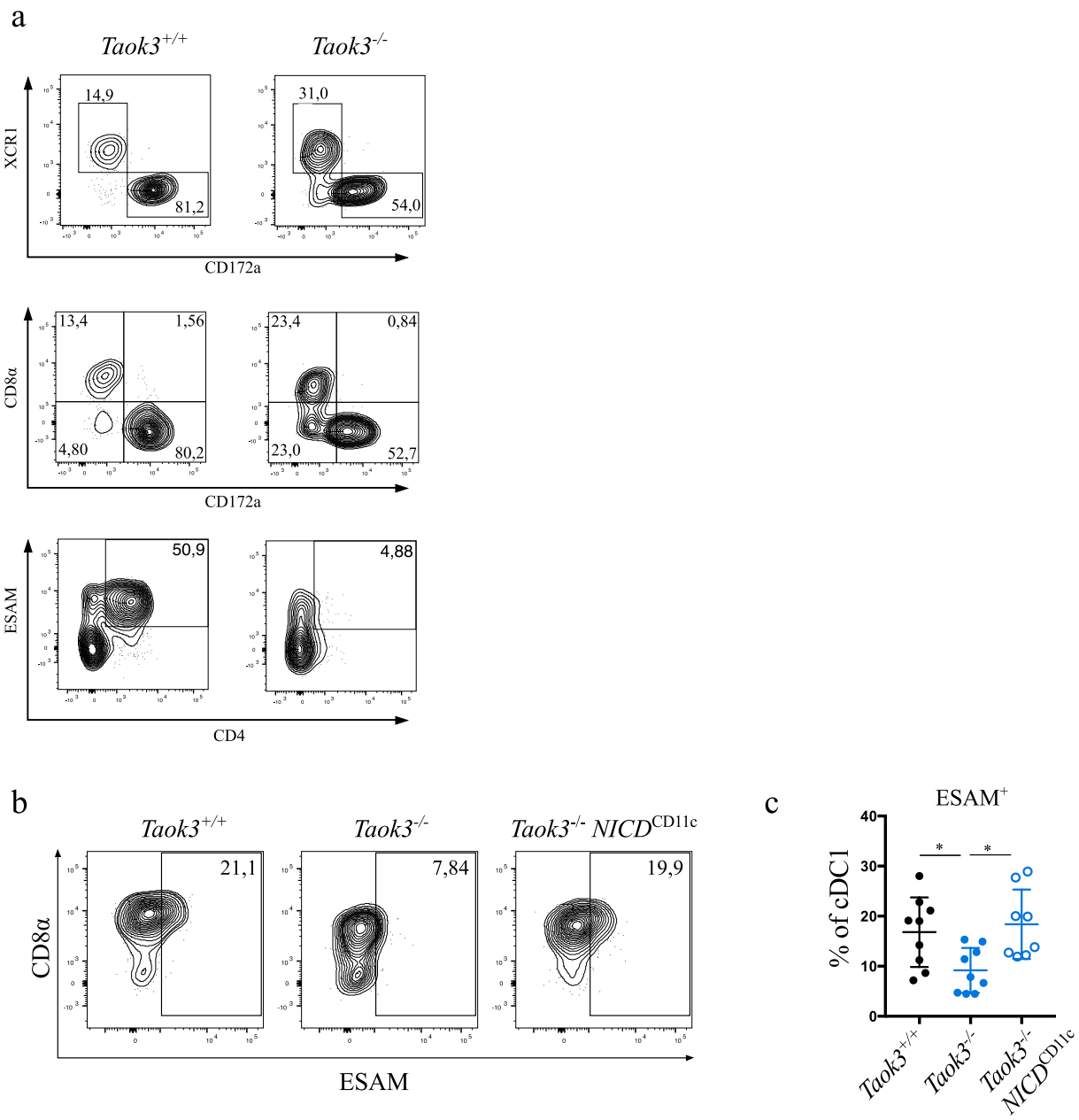


**Supplementary figure 10: ESAM expression is rescued by NICD overexpression in *Taok3*-deficient cDC1s.**
**(a)** Representative contour plots of splenic cDCs from *Taok3*$^{-/-}$ mice generated by CRISPR-CAS9 technology (see materials and methods) and littermate controls. Numbers adjacent to the gates denote percentage of total cDCs. **(b)** Representative plots of XCR1$^{+}$ splenic cDC1s from *Taok3*$^{-/-}$ *NICD*$^{CD11ccre}$ mice and littermate controls. Numbers within the gates indicate the percentage of total cDC1s. **(c)** Percentage of splenic cDC1s that express ESAM. Two sided Mann-Whitney U test. Bars indicate mean ± SD. * = p<0.05, ** = p<0.01, *** = p<0.001, **** = p<0.0001. (a-c) Data representative of at least 2 independent experiments (n=8-10 per group).